

## SCF in FRP strengthened tubular T-joints under brace axial loading, in-plane bending and out-of-plane bending moments

Alireza Sadat Hosseini<sup>1</sup>, Mohammad Reza Bahaari<sup>2</sup>, and Mohammad Lesani<sup>3</sup>

<sup>1</sup> School of Civil Engineering, College of Engineering, University of Tehran, Tehran, Iran

<sup>2</sup> School of Civil Engineering, College of Engineering, University of Tehran, Tehran, Iran

<sup>3</sup> School of Civil Engineering, College of Engineering, Sadra University, Tehran, Iran

**ABSTRACT:** Present research is dedicated to study the relative stress concentration factors (SCF) at FRP strengthened tubular T-joints subjected to brace axial loading, in-plane and out-of-plane bending moments using Finite Element Analyses performed by ABAQUS software package. Validation analysis for the finite element models of the unstiffened joints are performed against the Lloyd's Register and API equations together with the experimental results. The effectiveness of using three different types of FRP materials such as Glass/Vinyl ester, Glass/Epoxy (Scotch ply 1002) and Carbon/Epoxy (T300-5208) on enhancing the fatigue life of tubular T-joints through computing the SCFs was investigated. Promising results derived from analysis which show that this strengthening method can be considered as an effective method to lower the SCFs at T-joints.

### 1 INTRODUCTION

Offshore steel jackets are made by circular hollow sections (CHS) as load bearing members due to adequate structural performance of CHSs against bending, buckling and torsion and also another vantages such as high strength-to-weight ratio, high buoyancy and lower drag coefficients (Jia, 2008). Joints in offshore CHSs are usually made from connecting steel tubes using the butt welding technique. T-joints are the most common and basic CHS joint configuration which are made by welding the cross section of one tube (brace) perpendicular to the undisturbed exterior surface of the other tube (chord).

Offshore steel jacket structures are subjected to repeated loading and unloading cycles due to the cyclic nature of wave loading. Therefore, care must be given to fatigue phenomenon in such structures. Thus, prediction of fatigue life of offshore structural joints and accurate fatigue load resistance are necessary to ensure structural safety. Fatigue life of offshore structures is normally assessed using Stress-Life (S-N) curves. In this way, hot-spot stress range (HSSR) is calculated from a parameter called the stress concentration factor (SCF). According to API (2014)-Part 8.3.1, "For each tubular joint configuration and each type of brace loading, SCF is defined as: The hot spot stress range (HSSR)/nominal brace stress range". Here in this research we concentrated on estimation of SCFs at chord member. So, the HSSR is the hot spot stress range on the chord which must be divided by the nominal direct stress in the brace member to give the SCF. Having HSSR, and using S-N curves, the number of loading cycles that the structure can sustain before failure could be estimated.

SCFs can be considered in unstiffened and stiffened joints. In unstiffened joints, many researchers did efforts since the 1970s and their main objective was to derive parametric equations for the SCF calculation. Lesani et al. (2013) reviewed some of the strengthening techniques of CHSs. There are metallic as well as non-metallic external reinforcement schemes such as FRP strengthening technique. FRP wrapping method due to its convenience for handling and application, potentially high overall durability, corrosion resistance, light weight, superior strength-to-weight ratio, tailorability and high specific performance attributes with respect to steel, could be easier for application in areas which conventional materials may encounter durability, weight or lack of design flexibility constraints. As examples of studies on FRP strengthened steel structures, researches done by Hollaway and Cadei (2002), Zhao and Zhang (2007) and Zhao (2009) are remarkable. FRP-strengthened CHSs with four layers of CFRP under tension loading was investigated by Jiao and Zhao (2004). Zhao et al. (2006) studied the load bearing capacity of RHSs strengthened with CFRP sheets. Lesani et al. (2013) numerically investigated the failure pattern, ultimate static strength and detailed behavior of steel tubular T-joints strengthened by GFRP (Glass/epoxy) under axial brace compressive loading. Remarkable increase in joint ultimate capacity due to the combined action of steel and composite against the compressive load was observed. In addition, critical deformations and ovalization of chord member showed a descending trend up to 50% of the un-strengthened joint. Lesani et al. (2014) experimentally investigated the improvement of ultimate capacity of T-joints wrapped with GFRP (Glass/vinyl ester) under static compressive loading. Increase up to 50% in the ultimate load bearing capacity of the tubular joint strengthened by FRP was observed. A numerical and experimental research program was conducted by Lesani et al. (2015) on T and Y shaped CHS steel tubular connections strengthened with GFRP. This research showed numerically and experimentally that, the static strength of tubular joints could be improved significantly by the FRP wrapping technique. Based on the improvements observed in the static strength, investigation of SCF improvement and fatigue strength enhancement using the FRP wrapping technique seems to be necessary. The present research is aimed on such investigations on relative SCF values not addressed in previously studies. In this paper, the results of numerical analyses on FRP-strengthened steel tubular T-joints were used to present the effect of FRP material type on the SCF distribution along the weld toe under brace axial loading, and also the SCF values at crown and saddle positions under in-plane and out-of-plane bending moments respectively using Finite Element Analyses performed by ABAQUS software package. The finite element models of the unstiffened joints were verified against the experimental results extracted from HSE OTH 354 report (Health and Safety Executive (UK), 1997) and the predictions of Lloyd's Register (LR) (Health and Safety Executive (UK), 1997) and API (2014) equations. The results of analysis on stiffened finite element models could address how FRP properties can affect the SCF values and accordingly the fatigue life the strengthened T-joint under three major types of loadings.

## 2 FINITE ELEMENT MODELING AND VERIFICATION

Here, finite element models were developed and analysis were carried out using ABAQUS (2014) software package. The T-joints were chosen from JISSP project experimental results, the elastic stress concentration factor tests on tubular steel joints by Wimpey Offshore 1986 (Health and Safety Executive (UK), 1997), which are JISSP joint 1.3 (for axial loading) and JISSP joint 1.13 (for in-plane and out-of-plane bending moments). For more information about these joint refer to Health and Safety Executive (1997). Three types of common FRP materials, Glass/vinyl ester, Glass/epoxy (Scotch ply 1002) and Carbon/epoxy (T300-5208), are used as strengthening material on the T-joints in order to find out how FRP wrapping affects the SCF values through the parametric study. Table 1 demonstrates the properties of the FRP materials used in the

analyses. In this table, subscripts ‘‘1’’ and ‘‘2’’ stand for the fiber longitudinal and transverse directions respectively.

Table 1: FRP properties (Ganesh and Naik, 2005)

	$E_1$ (Mpa)	$E_2$ (MPa)	$\nu_{12}$	$G_{12}$ (MPa)	$G_{13}$ (MPa)	$G_{23}$ (MPa)
Glass/ Vinylester	28000	7000	0.29	4500	4500	2540
Glass/Epoxy (Scotch ply 1002)	38600	8270	0.26	4140	4140	3100
Carbon/Epoxy (T300-5208)	132000	10800	0.24	5700	5700	3400

In order to achieve accurate stresses along the chord-brace intersection, the weld profile should be modeled accurately. Here, the weld profile along the brace-chord intersection satisfies the specifications addressed in AWS (2010). In Figure 1(b) the weld profile section in finite element model can be seen. In this study, ABAQUS 3D brick elements are incorporated to model the joint geometry and weld profile after the sensitivity analysis. Element type C3D20 which is a 20-node quadratic brick is used to model the joint. FRP material is modeled using shell elements defined as a skin layer on the joint. ABAQUS element type S4R, which is a 4-node doubly curved thin or thick shell with reduced integration is used to model the FRP skin layers. FRP mesh elements are tied to the solid elements of the un-stiffened joint geometry, in other words, a perfect bond state was considered and no cohesive/adhesive element was modeled at the FRP and the steel substrate interface. This is not a irrational assumption since the bound between FRP layer and steel stays undisturbed in the elastic range of loading according to the experimental and numerical analysis by Lesani et al. (2014).

Different sub-zone mesh generation methods was used for the weld profile, hot spot stress region, FRP wrapping area and other regions of the joint. The mesh in the hot-spot stress region is much finer than the other zones since more computational precision is required in this area. FRP wrapping areas have coarser meshes but still fine enough to ensure computational accuracy. Figure 1 shows the mesh generated for the tubular T-joint.

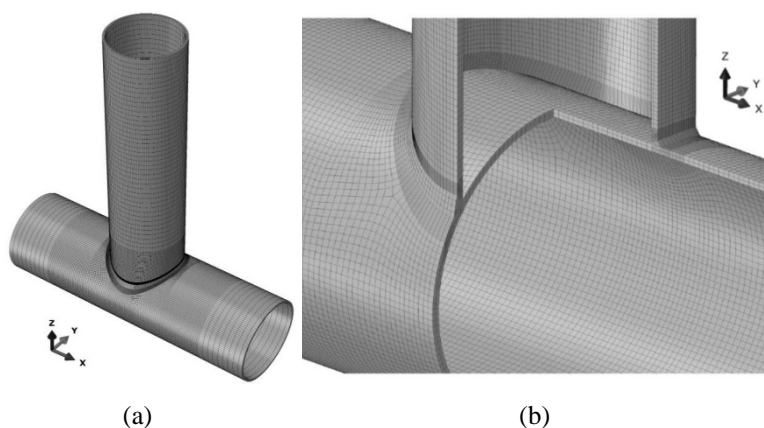


Figure 1. The mesh generated for the T-joint (JISSP joint 1.13) using the sub-zone method: a) Isometric view; b) Mesh enlargement

As previously mentioned, the tubular T-joints in this study are modeled based on the joint properties given in JISSP project (Health and Safety Executive (UK), 1997). Thus, all the brace and chord geometry details are modeled according to JISSP joint 1.3 for axial loading and JISSP joint 1.13 for IPB (in-plane bending) and OPB (out-of-plane bending) moments.

The boundary conditions are chosen in such a way to represent the actual boundary conditions of the experiment. Here in the analyses, chord ends were assumed to be fixed.

In order to determine the stress concentration factors in a tubular joint, a linear elastic numerical analysis needs to be performed (N'Diaye et al., 2007). The Young's modulus and Poisson's ratio of steel are taken as 207 GPa and 0.3, respectively. In order to estimate the SCFs, the method introduced by IIW-XV-E is implemented. In this method, the peak stress at the weld toe is calculated by linear extrapolating the von-Mises stresses at distances of 0.4T and 1.4T from the weld toe; where T is the thickness of the chord member. SCF is calculated by dividing the von Mises stresses at weld toe by the nominal stress in the brace.

In order to validate the finite element model, Lloyd's Register equations and API equations for SCF computation together with the test results published in HSE OTH 354 report for JISSP joint 1.3 and 1.13 were used. Table 2 summarizes the verification results at the saddle and crown points. In this table,  $e_1$  and  $e_2$  show the percentage of relative difference of Lloyd's Register and API equations with test results respectively, and  $e_3$  denotes the percentage of relative difference between the results of finite element model and the experiment results. According to Table 2, it is obvious that the finite element model predicts the SCFs at crown and saddle points accurately which is in good agreement with the test results and therefore, the FE model is validated.

Table 2 - Comparison of finite element results with experimental data (Health and Safety Executive (UK), 1997) and predictions of Lloyd's Register (LR) and API equations

Reference	D (mm)	$\alpha$	$\beta$	$\gamma$	$\tau$	Load / Position	Test	LR Eq.	API Eq.	FEM	$e_1$ (%)	$e_2$ (%)	$e_3$ (%)
JISSP joint 1.3	508	10	0.8	20.3	0.99	AX / Crown	5.4	3.94	3.85	5.3	27.0	28.7	1.9
						AX / Saddle	11.4	10.54	12.13	11.1	7.5	6.4	2.6
JISSP joint 1.13	508	6.2	0.8	20.3	1.07	IPB / Crown	3.9	4.07	4.85	3.92	4.4	24.4	0.5
						OPB / Saddle	12.2	18.2	15.3	10.1	49.2	25.4	-17.2

Where D is the chord diameter;  $\alpha=2L/D$ , L is the chord length;  $\beta=d/D$ , d is the brace diameter;  $\gamma=D/2T$ , T is the chord thickness;  $\tau=t/T$ , t is the brace thickness.

### 3 ANALYSIS AND RESULTS

Here the analyses and results on the strengthened joints are explained. In order to investigate the stress concentration in FRP strengthened tubular T-joints under the three types of loadings, models were generated and analyzed using ABAQUS finite element software package. Stresses along the chord-brace intersection and correspondingly the SCF values could strongly be affected by change in FRP mechanical properties due to change in fiber and/or matrix material. The three mentioned FRP materials (Glass-vinyl ester, Glass-epoxy and Carbon-epoxy) were used for strengthening. Analyses were carried out in three phases. At first, the chord alone was strengthened in order to investigate the effects of strengthening the chord member on SCFs (Figure 2(a)). In the second phase, FRP was applied only on the brace member to study the brace strengthening effects (Figure 2(b)), and finally in the third phase, both of the chord and brace members were strengthened (Figure 2(c)). In case of axial loading the SCF values are presented along the chord-brace intersection but for the IPB and OPB moments, due to the asymmetry in the loading, SCFs are calculated only in Crown and Saddle points. The details and

results of the analyses on SCF values in strengthened T-joints for each type of loading are as follow.

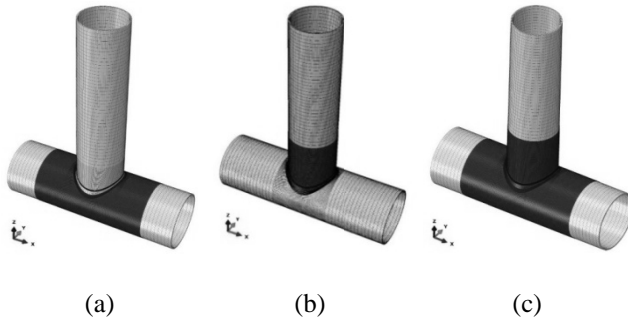


Figure 2. A typical FRP wrapped T-joint: a) Chord strengthening; b) Brace strengthening; c) Chord and brace strengthening

### 3.1 Axial loading

Here the effect of FRP mechanical properties through analyzing the FRP strengthened T-joint (JISSP joint 1.3) for the three types of FRP materials on SCF distribution along chord-brace intersection were investigated. Figure 3 shows the relative SCFs ( $SCF_s$ : SCF at strengthened joint divided by  $SCF_u$ : SCF at unstiffened joint). This stress distribution is symmetric under axial loading in a T-joint. Thus, results are presented along a 90 degree polar angle (a quarter of Chord-Brace intersection zone) which starts from the Crown point and ends at the Saddle point.

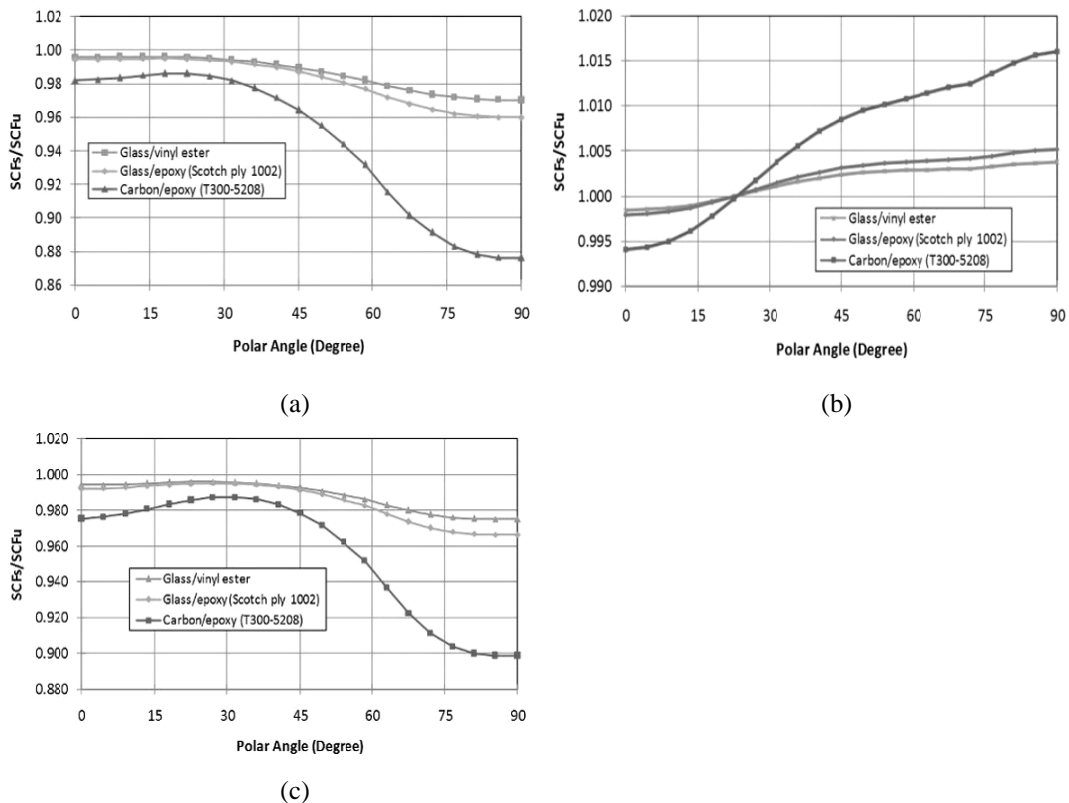


Figure 3. Ratio of SCF distribution in FRP strengthened tubular T-joint with different FRP materials to SCF distribution in un-strengthened joint: a) Chord member is strengthened; b) Brace member is strengthened; c) Both chord and brace are strengthened

The strengthening materials are applied on the T-joint with  $0^\circ$  orientation fibers (Chord hoop direction and along brace longitudinal axis), having a thickness of 1 mm and a wrapping length equal to one diameter of the relative strengthened member. The effects of FRP material properties when only the chord member is strengthened are presented in Figure 3(a). More stiffer FRP material (Higher mechanical properties) shows more effectiveness in decreasing the SCF values. As clearly envisaged from this figure, using carbon-epoxy material has effectiveness of about three times the GFRP material on SCF reduction, which is about 12% at the Saddle point. As previously stated, strengthening the brace member has an increasing effect on SCFs for polar angles between  $20^\circ$  and  $90^\circ$  (Saddle point) and adverse effect for  $0^\circ$  (Crown point) to  $20^\circ$ . These effects are amplified by increasing the mechanical properties of FRP materials (Figure 3(b)). The adverse effect of using higher modulus materials on brace member only, is about maximum 1.6% at the saddle point. Figure 3(c) presents the effect of different FRP material on SCF values when the chord and brace are both strengthened in a T-joint. Based on this figure, adverse effects from chord and brace strengthening compromise each other in various polar angles. Thus, the maximum effectiveness of the 1mm thick FRP with Carbon-epoxy material and  $0^\circ$  fiber orientation is about 10 percent at the Saddle point.

### 3.2 IPB and OPB moments

In this section, effects of using the three strengthening materials on SCF values at crown and saddle points of a T-joint (JISSP joint 1.13) were investigated subject to IPB and OPB loadings. Similar to the strengthening scheme for axial loading, in all models, the FRPs have a thickness of 1 mm, wrapping length equal to the diameter of the relative strengthened member (1D for chord member and 1d for brace member, where D and d are the chord and brace diameters respectively).

FRP materials were applied on the joint fibers in both  $0^\circ$  and  $90^\circ$  orientations. The effects of FRP material when the chord member, the brace member, and both chord and brace members were strengthened are presented in Figure 4(a) and 4(b) for IPB and OPB loadings respectively. In these figures, for instance, Ch0 stands for the strengthened chord which has  $0^\circ$  fiber orientation and Br90 is the strengthened brace with  $90^\circ$  fibers orientation. When both chord and brace members were strengthened, for instance, "Ch0Br90" is a synthetic strengthened joint (Both chord and brace members were stiffened) with  $0^\circ$  fibers orientation at chord and  $90^\circ$  fibers orientation at brace. In other words, the chord and brace FRP fibers are along the transverse (hoop) direction. According to Figure 4(a), in case of IPB loading, when only the chord member was strengthened with  $90^\circ$  fibers, the SCF values were reduced effectively, while for OPB loading, according to Figure 4(b), the most decreasing effect on SCFs was observed when fibers were placed in  $0^\circ$  orientation in the strengthened chord. Brace strengthening had an adverse effect on SCF values. Besides, change in material properties shows more considerable alteration on SCF values when FRP fibers are in  $90^\circ$  and  $0^\circ$  in IPB and OPB loadings respectively. Focusing on these figures reveals that the strengthened brace with  $0^\circ$  fibers has the highest decreasing effect on the SCF amplitude.

Having Figure 4(a) and 4(b) along with the mechanical properties given in Table 1, one can find how the change in value of each mechanical property in two main extreme fiber orientations ( $0^\circ$  and  $90^\circ$ ) will affect the SCFs.

As depicted from figure 4, the effectiveness enhances by using stiffer composite material. Moreover, using carbon-epoxy material has higher effectiveness in comparison to the GFRP

material on SCF reduction. Generally, it is revealed that among four different schemes of  $0^\circ$  and  $90^\circ$  fibers orientation for synthetic schemes, when the chord member is strengthened with  $0^\circ$  fibers in the FRP system and the brace member with  $90^\circ$  (Ch0&Br90), the most reducing effect on SCF values is observed. As an example, using this scheme with Carbon-epoxy FRP material, SCFs are decreased by 11.2% for IPB loading and 14.6% for OPB loading.

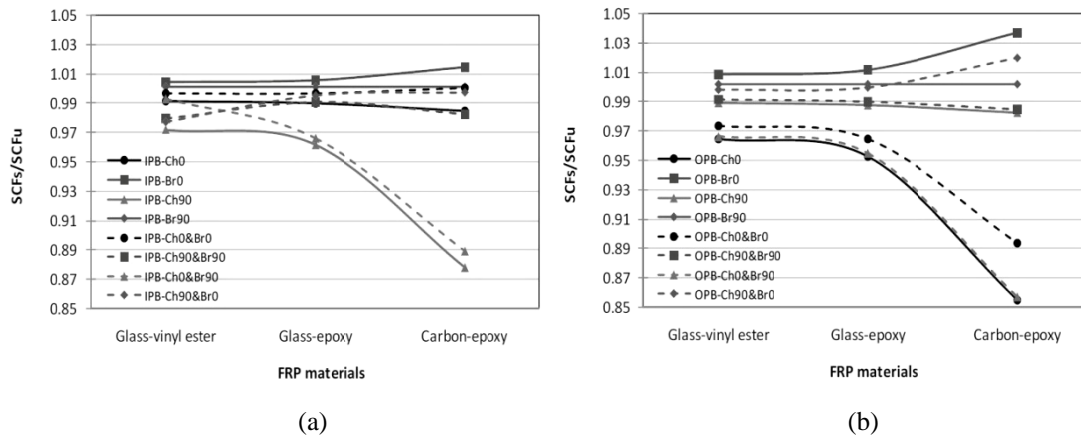


Figure 4. Ratio of SCF distribution in FRP strengthened tubular T-joint with different FRP materials to SCF distribution in un-strengthened joint: a) In-plane bending moment; b) Out-of-plane bending moment

#### 4 SUMMARY AND CONCLUSIONS

In this research, changes in SCF values at  $90^\circ$  polar angle in one quarter of the Chord-Brace intersection area in an axially loaded tubular T-joint due to change in FRP material used for wrapping the joint was investigated. In addition, SCF alteration at the Crown and Saddle positions of the Chord-Brace intersection area under IPB and OPB moments was studied. Models were verified based on experimental data gathered from the JISSP project. The following conclusions were derived from this study.

In case of Axial loading:

- Change of fiber and/or matrix material properties corresponds to change in FRP mechanical properties. Use of FRP material with higher values of mechanical properties are more effective in lowering the SCF values. Among the common composite material, carbon-epoxy has effectiveness of about three times the glass-vinyl ester in SCF reduction.
- Due to the better fatigue performance of CFRP materials in comparison to other composite materials such as GFRP, and based on the findings of this study, it is recommended to use CFRP composites as wrapping and strengthening material for fatigue life extension of tubular joints. Anyway, economical issues must be addressed.

In case of IPB and OPB moments:

- Generally, more decrease in SCF values observed when stiffer FRP materials are used for strengthening.
- In case of IPB loading, the most decreasing effect on SCFs was observed when only the chord member is strengthened with  $90^\circ$  orientation of fibers.

- In case of OPB loading, use of FRP wrapping with  $0^\circ$  orientation of fibers only on the chord member has the most falling effect on SCFs. Brace strengthening has unfavorable results on SCFs in both IPB and OPB loading conditions, as when the fibers are in  $0^\circ$  orientation, the worst effect was observed.
- Generally, results of SCFs for strengthening both chord and brace members stand between the results of individual chord or brace strengthening. As an interesting result, among the synthetic schemes (Strengthening both chord and brace members), when the chord and brace fibers are in  $0^\circ$  and  $90^\circ$  orientations respectively, the most effective result on downsizing the SCFs values was observed in both IPB and OPB loading conditions.

Further numerical and experimental investigations would be necessary to achieve more understandings about SCF values in FRP strengthened joints.

## 5 REFERENCES

- ABAQUS/CAE Standard user's manual-Version 6.14-1. 2014.
- API (American Petroleum Institute). 2014. Recommended practice for planning, designing and constructing fixed offshore platforms - working stress design, API RP 2A WSD. 22nd edition.
- AWS (American Welding Society). 2010. Structural welding code, AWS D 1.1:2010 (22nd Edition). Miami, FL (USA), American Welding Society, Inc.
- Ganesh, K, Naik, NK. 2005. Some strength studies on FRP laminates. *Journal of Composite Structures*,24,51-8.
- Health and Safety Executive (UK). 1997. OTH 354: Stress concentration factors for simple tubular joints - assessment of existing and development of new parametric formulae. Prepared by Lloyd's Register of Shipping.
- Hollaway, LC, Cadei, J. 2002. Progress in the technique of upgrading metallic structures with advanced polymer composites. *Progress in Structural Engineering and Materials*, 4(2),131-48.
- IIW-XV-E. 1999. International institute of welding sub-commission XV-E, recommended fatigue design procedure for welded hollow section joints. IIW Docs, XV-1035-99/XIII-1804-99. International Institute of Welding, France.
- Jia, J. 2008. An efficient nonlinear dynamic approach for calculating wave induced fatigue damage of offshore structures and its industrial applications for lifetime extension. *Applied Ocean Research*,30,189-98.
- Jiao, H, Zhao, XL. 2004. CFRP strengthened butt-welded very high strength (VHS) circular steel tubes. *Thin-Walled Structures*,42(7),963-78.
- Lesani, M, Bahaari, MR, Shokrieh, MM. 2013. Numerical investigation of FRP-strengthened tubular T-joints under axial compressive loads. *Composite Structures*,100,71-8.
- Lesani, M, Bahaari, MR, Shokrieh, MM. 2014. Experimental investigation of FRP-strengthened tubular T-joints under axial compressive loads. *Construction and Building Materials*,53,243-52.
- Lesani, M, Bahaari, MR, Shokrieh, MM. 2015. FRP wrapping for the rehabilitation of Circular Hollow Section (CHS) tubular steel connections. *Thin-Walled Structures*,90,216-234.
- N'Diaye, A, Hariri, S, Pluvinage, G, Azari, Z. 2007. Stress concentration factor analysis for notched welded tubular T-joints. *International Journal of Fatigue*,29,1554-70.
- Zhao, XL, Fernando D, Al-Mahaidi R. 2006. CFRP strengthened RHS subjected to transverse end bearing force. *Engineering Structures*,28(11),1555-65.
- Zhao, XL, Zhang, L. 2007. State of the art review on FRP strengthened steel structures. *Engineering Structures*,29(8),1808-23.
- Zhao, XL. 2009. FRP strengthened metallic structures. *Thin Walled Structures*, Special Issue,47(10),1019.